Modeling Rotating Stratified Turbulent Flows with Application to Oceanic Mixed Layers

B. GALPERIN,*,† A. ROSATI,** L. H. KANTHA* AND G. L. MELLOR*

*Program in Atmospheric and Oceanic Sciences, Princeton University, Princeton, New Jersey;
**Geophysical Fluid Dynamics Laboratory/NOAA, Princeton University, Princeton, New Jersey

(Manuscript received 4 April 1988, in final form 27 December 1988)

ABSTRACT

Rotational effects on turbulence structure and mixing are investigated using a second-moment closure model. Both explicit and implicit Coriolis terms are considered. A general criterion for rotational effects to be small is established in terms of local turbulent Rossby numbers. Characteristic length scales are determined for rotational effects and Monin–Obukhov type similarity theory is developed for rotating stratified flows. A one-dimensional version of the closure model is then applied to simulate oceanic mixed layer evolution. It is shown that the effects of rotation on mixed layer depth tend to be small because of the influence of stable stratification. These findings contradict a hypothesis of Garwood et al. that rotational effects on turbulence are responsible for the disparity in the mixed-layer depths between the eastern and western regions of the equatorial Pacific Ocean. The model is also applied to neutrally stratified flows to demonstrate that rotation can either stabilize or destabilize the flow.

1. Introduction

The role of rotational terms in the balance of the second-order turbulence correlations in geophysical flows has not been thoroughly investigated to date, although the need for such a study has often been acknowledged (Mellor 1973; Zeman and Tennekes 1975; Mellor and Yamada 1982). When Coriolis terms are nonzero, inherent algebraic complexity involved in obtaining explicit relationships for turbulent exchange coefficients in the framework of higher-order turbulence closure models has hindered a systematic study of rotational effects. Generally, Coriolis terms have been assumed small and neglected in the second moment equations (Mellor 1973; Mellor and Yamada 1982). However, recent studies by Garwood et al. (1985a,b) suggest that these terms may not always be small and may play a significant role. Their analysis is based on an extension of the vertically integrated, bulk mixed layer model by Garwood (1977) that includes Coriolis terms in the equations for turbulence energy components; the model neglects off-diagonal elements in the Reynolds stress tensor. Garwood et al. (1985b) applied their model to the mixed layer in the equatorial western Pacific Ocean and attributed its unusually large depth to the redistribution of turbulence energy from the horizontal to the vertical component due to the action of the poleward component of the Coriolis vector, f_y. Their model presumably accounts for the difference in mixed layer depths in the western and eastern parts of the equatorial Pacific Ocean on the basis of differences in the atmospheric forcing and the effect of the terms proportional to f_y. (Curiously, they posit an equilibrium equatorial mixed layer and neglect consideration of the momentum equation. However, consideration of that equation at 0° latitude and for horizontally homogeneous fields indicates that an equilibrium mixed layer is not possible as illustrated by the experiments of Kato and Phillips 1969 and Kantha et al. 1977.) This finding is important for equatorial oceanography and one of the goals of the present study is to verify whether or not the same conclusion would be supported by a local, second moment turbulence closure model rather than a bulk model.

In second-moment models the explicit effect of Coriolis terms in the equations for Reynolds stress and heat flux components need not be modeled; they are linear functions of the stresses and fluxes themselves. Therefore, no new modeling assumptions are needed. We here merely overcome analytical complexity in extending a second moment model into parameter space where the Coriolis effect is liable to be important. It is true that additional, implicit Coriolis terms could be included in, for example, the Rotta hypothesis for the pressure, rate of strain covariance terms, but in section 3 we exclude these terms; their inclusion would decrease the total Coriolis effect and we wish here to establish an upper bound to this effect.

In this paper the direct effects of the vertical and

† Present affiliation: Program in Applied and Computational Mathematics, Princeton University.

Corresponding author address: Dr. B. Galperin, Program in Applied and Computational Mathematics, Princeton University, Princeton, NJ 08544.

poleward component of rotation on turbulence structure is studied using the level 2½ closure model by Mellor and Yamada (1982) as operationally modified by Galperin et al. (1988). However, as already stated, the same explicit Coriolis terms appear automatically in all second-moment closure schemes and the relative effect of the terms should not differ essentially among this class of models.

The importance of Coriolis terms has been recognized in a variety of other contexts, particularly in rotating turbomachinery, where flows around compressor or turbine blades are also subject to rotational effects (an excellent review was given by Bradshaw 1973). A number of experiments have been designed to study this kind of flow with engineering applications in mind. Among them are the experiments by Johnston et al. (1972) on rotating duct flows (so-called "spanwise" rotation), and Koyama et al. (1979) and Watmuff et al. (1985) on spanwise rotating boundary layer flows. These experiments allow one to compare flows with and without rotation and extract information unavailable in a geophysical context. A recent review of numerical modeling activity in these fields is given by Lakshminarayana (1986). In particular, he shows that local models of the type used in this study provide a good description of rotating flows. One should note that flows of engineering importance are generally not stratified but they are affected by other complicating factors, such as three-dimensionality, compressibility, and so on.

In the present work, the problem of algebraic complexity in the framework of a local model has been addressed both by straightforward calculations and by the use of a symbolic computer language, REDUCE, which is capable of performing complicated algebraic manipulations and producing Fortran instructions for insertion into numerical code.

In the simpler cases of neutral or weakly stratified flows, explicit expressions for exchange coefficients are derived and further analysis is performed using the approximation of local equilibrium.

The paper is organized as follows: section 2 provides the mathematical formulation of a turbulence closure model which is a modification by Galperin et al. (1988) of the Mellor and Yamada (1982) level 2½ model, but now accounting for the effects of rotation on the second-order turbulence correlations. A discussion of the length scale of turbulence, l, is also presented. In section 3, explicit and implicit Coriolis terms are defined and analyzed. Section 4 describes different approaches to handle the set of algebraic equations of the problem and provides a general analysis of these equations. It is shown that stable stratification strongly suppresses rotational effects on turbulence. Section 5 introduces the length scales characterizing rotational effects via local equilibrium and constant flux layer analyses. Monin–Obukhov type similarity theory is developed to study the combined effects of rotation and stratification and the limit is considered in which both factors are small. Section 6 deals with the application of the model to oceanic mixed layers, specifically to study the effects of rotation on a one-dimensional wind driven oceanic mixed layer developing in a stably stratified environment. The relevance of these results to the hypothesis of Garwood et al. (1985b) is discussed. Finally, section 7 presents some concluding remarks. In addition, appendix A addresses neutral flows where rotational phenomena are investigated analytically. Some of the effects specific to rotation as well as some geophysical aspects of the problem are emphasized.

2. Mathematical formulation of the problem

We shall begin with a set of equations describing stratified turbulent flows in a rotating coordinate frame under Boussinesq approximation using a quasi-equilibrium modification by Galperin et al. (1988) of the Mellor and Yamada (1982) level 2½ model. Those equations are

the continuity equation:

$$\frac{\partial U_i}{\partial x_i} = 0, \tag{1}$$

the momentum equation:

$$\frac{DU_i}{Dt} + \epsilon_{ikl} f_k U_l = \frac{1}{\rho_0}\frac{\partial}{\partial x_l}(-\overline{u_i u_l}) - \frac{1}{\rho_0}\frac{\partial P}{\partial x_i} - g_i\frac{\rho}{\rho_0}, \tag{2}$$

and the energy equation:

$$\frac{D\Theta}{Dt} = \frac{\partial}{\partial x_l}(-\overline{u_l\theta}), \tag{3}$$

where U_i and u_i are mean and fluctuating velocities, Θ and θ are mean and fluctuating potential temperature, ρ_0 is reference density, P is mean pressure, $f_k = 2\Omega_k$ is the Coriolis vector, where Ω_k is the angular velocity vector of the Earth, and $f_k = (0, f_y, f)$; $g_i = (0, 0, -g)$ is the acceleration due to gravity. The model equations for turbulence quantities are

the Reynolds stress equation:

$$\overline{u_i u_j} = \frac{\delta_{ij}}{3}q^2 - \frac{3l_1}{q}\left[\overline{u_k u_i}\frac{\partial U_j}{\partial x_k} + \overline{u_k u_j}\frac{\partial U_i}{\partial x_k} - C_1 q^2\left(\frac{\partial U_i}{\partial x_j} + \frac{\partial U_j}{\partial x_i}\right) + \beta(g_i\overline{u_j\theta} + g_j\overline{u_i\theta}) + f_k(\epsilon_{ikl}\overline{u_l u_j} + \epsilon_{jkl}\overline{u_l u_i}) + \frac{2q^3}{3\Lambda_1}\delta_{ij}\right], \tag{4}$$

the heat flux equation:

$$\overline{u_i\theta} = -\frac{3l_2}{q}\left[\overline{u_i u_k}\frac{\partial\Theta}{\partial x_k} + \overline{\theta u_k}\frac{\partial U_i}{\partial x_k} + \beta g_i\overline{\theta^2} + f_k\epsilon_{ikl}\overline{u_l\theta}\right], \tag{5}$$

the turbulence energy equation:

$$\frac{Dq^2}{Dt} - \frac{\partial}{\partial x_k}\left(qlS_q \frac{\partial q^2}{\partial x_k}\right) = -2\overline{u_k u_l}\frac{\partial U_k}{\partial x_l} - 2\beta g_k \overline{u_k \theta} - 2\frac{q^3}{\Lambda_1}, \quad (6)$$

and the temperature variance equation:

$$\overline{\theta^2} = -\frac{\Lambda_2}{q}\overline{u_k\theta}\frac{\partial \Theta}{\partial x_k}. \quad (7)$$

Here $\beta = -(\partial\rho/\partial T)_p/\rho_0$, the thermal expansion coefficient, S_q is the nondimensional vertical exchange coefficient for turbulence kinetic energy, $q^2 = \overline{u_k^2}$, and various length scales of turbulence are related to the master length scale, l, following Mellor and Yamada (1982):

$$(l_1, l_2, \Lambda_1, \Lambda_2) = (A_1, A_2, B_1, B_2)l, \quad (8)$$

where

$$(A_1, A_2, B_1, B_2) = (0.92, 0.74, 16.6, 10.1). \quad (9)$$

It can be shown (Mellor 1975) that the remaining constant, C_1, is related to the others according to

$$C_1 = \tfrac{1}{3}(1 - 6A_1B_1^{-1} - A_1^{-1}B_1^{-1/3}) = 0.08. \quad (10)$$

The master length scale, l, is given by the q^2l equation (Mellor and Yamada 1982):

$$\frac{Dq^2l}{Dt} - \frac{\partial}{\partial x_k}\left[qlS_q\frac{\partial}{\partial x_k}(q^2l)\right] = lE_1\left(-\overline{u_k u_l}\frac{\partial U_k}{\partial x_l} - \beta g_k\overline{u_k\theta}\right) - \frac{q^3}{B_1}\left[1 + E_2\left(\frac{l}{\kappa L}\right)^2\right], \quad (11)$$

where $E_1 = 1.8$, $E_2 = 1.33$, L is a measure of the distance away from a nondeforming surface, and κ is the von Kármán constant ($\kappa = 0.4$). The oceanic free surface is considered to be—perhaps simplistically—a nondeforming surface.

Equation (11) is an empirical equation which is related to the integral of the two-point correlation functions. It behaves correctly in the case of grid-generated, decaying turbulence and seems to provide a reasonable length scale in the case of neutral or stratified boundary layers. However, if Eqs. (4) and (5) are written nondimensionally, one encounters the Coriolis terms appearing in the form, $f_k l/q = (0, f_y l/q, fl/q)$, and it becomes a matter of importance as to how l/q behaves at the edge of a stratified boundary layer. The present model invariably produces $q \to 0$ while $l \to$ constant as one proceeds from the shear driven, active turbulence region to the stratification dominated region and therefore $f_k l/q \to \infty$ at the edge of the turbulent boundary layer. However, there is evidence, cited below, that when high Reynolds number turbulence decays spatially or temporally to internal waves due to a stable stratification the cascade process ceases and turbulent fluxes and dissipation become negligible. Then the turbulence length scale is bounded according to

$$lN/q \leqslant c, \quad (12)$$

where

$$N = [-g(\partial\rho/\partial z)/\rho_0]^{1/2}$$

is the Brunt–Väisälä frequency, and c is an empirical constant. Experimental and observational studies of shear, shear-free and grid-generated turbulent flows developing in a stably stratified environment generally support the constraint (12) (for a review, see Hopfinger 1987). However, there is an ambiguity as to the value of the numerical constant, c. Various length scales have been introduced to characterize the limiting influence of stable stratification on turbulent eddies but it is not clear a priori how these scales are related to the model macroscale, l. Two relevant scales are the Ozmidov (1965) or Dougherty (1961) length scale,

$$L_R = (\epsilon/N^3)^{1/2}, \quad (13a)$$

where ϵ is the dissipation rate given in the model by

$$\epsilon = q^3/B_1 l, \quad (14)$$

and the Ellison (1957) length scale,

$$L_t = \rho'/(\partial\rho/\partial z), \quad (13b)$$

where ρ' is the rms of the density fluctuations. The inverse of L_R is related to the buoyancy wavenumber separating turbulence ($k^{-5/3}$) and buoyancy (k^{-3}) parts of the energy spectrum (Phillips 1977). On the other hand, L_t characterizes a vertical distance traveled by a fluid particle before either overturning or returning to the equilibrium position. Itsweire et al. (1986) point out that length scales of the largest overturns might be two to three times larger than L_t. Experiments by Stillinger et al. (1983) on grid turbulence in a water tunnel, measurements by Dillon (1982) in seasonal lake and ocean thermocline and estimations by Crawford (1986) using the data from the thermocline in the tropical Pacific Ocean suggest that

$$L_t = (0.7 \pm 0.2)L_R. \quad (15)$$

Starting with the square root of Eq. (19), presented below, in place of the right-hand side of (13b), one finds with the help of several model equations that $c = 0.28 \pm 0.11$. On the other hand, Dickey and Mellor (1980) in their experiments on decaying turbulence in stably stratified fluids found $lN/q \approx 0.6$ at the late stages of the decay. Andre et al. (1978), Hassid and Galperin (1983) and Galperin et al. (1988) used $c = 0.53$ in their simulations of turbulence entrainment into a stably stratified environment. Therefore, it is reasonable to assume that the numerical value of the

coefficient, c, in the constraint (12) should be somewhere between 0.3 and 0.6, which agrees with the value, 0.53, used in the above mentioned numerical simulations. The inequality (12) with $c = 0.53$ was used in the present model as an overriding constraint on Eq. (11) although that equation could have been altered to incorporate (12) directly. Note that this constraint also implies $\epsilon \propto N$ in stably stratified flows, in agreement with recent estimations of ϵ from direct measurements of small-scale shear in the upper ocean (Gargett and Osborn 1981; Leuck et al. 1983). We shall see in section 4 that this limitation also plays a crucial role in damping rotational effects by stable stratification.

When the boundary layer approximation is invoked, Eqs. (4)–(7) may be written

$$\begin{bmatrix} \overline{uv} \\ \overline{uw} \\ \overline{vw} \end{bmatrix} = -\frac{3l_1}{q} \begin{bmatrix} \overline{uw}\,\dfrac{\partial V}{\partial z} + \overline{vw}\,\dfrac{\partial U}{\partial z} \\ (\overline{w^2} - C_1 q^2)\dfrac{\partial U}{\partial z} - \beta g \overline{u\theta} \\ (\overline{w^2} - C_1 q^2)\dfrac{\partial V}{\partial z} - \beta g \overline{v\theta} \end{bmatrix} - \frac{3l_1}{q} \begin{bmatrix} f_y \overline{vw} + f(\overline{u^2} - \overline{v^2}) \\ -f\overline{vw} + f_y(\overline{w^2} - \overline{u^2}) \\ -f_y \overline{uv} + f\overline{uw} \end{bmatrix}, \quad (16)$$

$$\begin{bmatrix} \overline{u\theta} \\ \overline{v\theta} \\ \overline{w\theta} \end{bmatrix} = -\frac{3l_2}{q} \begin{bmatrix} \overline{uw}\,\dfrac{\partial \Theta}{\partial z} + \overline{w\theta}\,\dfrac{\partial U}{\partial z} \\ \overline{vw}\,\dfrac{\partial \Theta}{\partial z} + \overline{w\theta}\,\dfrac{\partial V}{\partial z} \\ \overline{w^2}\,\dfrac{\partial \Theta}{\partial z} - \beta g \overline{\theta^2} \end{bmatrix} - \frac{3l_2}{q} \begin{bmatrix} f_y \overline{w\theta} - f\overline{v\theta} \\ f\overline{u\theta} \\ -f_y \overline{u\theta} \end{bmatrix}, \quad (17)$$

$$\begin{bmatrix} \overline{u^2} \\ \overline{v^2} \\ \overline{w^2} \end{bmatrix} = \frac{q^2}{3}\left(1 - \frac{6A_1}{B_1}\right)\begin{bmatrix} 1 \\ 1 \\ 1 \end{bmatrix} - \frac{3l_1}{q} \begin{bmatrix} 2\overline{uw}\,\dfrac{\partial U}{\partial z} \\ 2\overline{vw}\,\dfrac{\partial V}{\partial z} \\ -2\beta g \overline{w\theta} \end{bmatrix} - \frac{6l_1}{q} \begin{bmatrix} f_y \overline{uw} - f\overline{uv} \\ f\overline{uv} \\ -f_y \overline{uw} \end{bmatrix}, \quad (18)$$

$$\overline{\theta^2} = -\frac{B_2 l}{q}\,\overline{w\theta}\,\frac{\partial \Theta}{\partial z}. \quad (19)$$

3. Explicit and implicit Coriolis terms

The Reynolds stress and heat flux equations (4) and (5) developed in the previous section include the explicit Coriolis terms,

$$R_{ij}^E \equiv f_k(\epsilon_{ikl}\overline{u_l u_j} + \epsilon_{jkl}\overline{u_l u_i}) \quad (20a)$$

$$H_i^E \equiv \epsilon_{ikl} f_k \overline{u_l \theta}. \quad (21a)$$

The process of derivation of Eqs. (4) and (5) was based on the Rotta hypothesis for pressure, rate of strain covariance terms which could be extended to include additional implicit Coriolis terms. A generalization of the Rotta hypothesis (Zeman and Tennekes 1975) yields implicit Coriolis terms as follows:

$$R_{ij}^I = -\alpha_1 f_k(\epsilon_{ikl}\overline{u_l u_j} + \epsilon_{jkl}\overline{u_l u_i}), \quad (20b)$$

$$H_i^I = -\alpha_2 \epsilon_{ikl} f_k \overline{u_l \theta}, \quad (21b)$$

where α_1 and α_2 are numerical constants. Therefore, the total contribution of Coriolis terms will be

$$R_{ij} = R_{ij}^E + R_{ij}^I = (1 - \alpha_1) f_k(\epsilon_{ikl}\overline{u_l u_j} + \epsilon_{jkl}\overline{u_l u_i}), \quad (20c)$$

$$H_i = H_i^E + H_i^I = (1 - \alpha_2)\epsilon_{ikl} f_k \overline{u_l \theta}. \quad (21c)$$

Zeman and Tennekes (1975) have found the coefficients, α_1 and α_2, to be positive, but they also mentioned that Lumley has found α_1 to be a small negative number, -0.06. Thus, the implicit terms are likely to be unimportant or to reduce the total effect of the Coriolis terms. In this study, however, we shall assume that $\alpha_1 = \alpha_2 = 0$ thus neglecting the implicit Coriolis terms and, possibly, overestimating the effect of rotation on turbulence.

It is useful to notice that both explicit and implicit Coriolis terms have zero trace and, therefore, they do not alter the turbulence energy.

4. Method of solution

When rotational effects are not considered, the set of algebraic equations (16)–(19) of the level 2½ model admits eddy viscosity–eddy diffusivity formulation:

$$-\begin{bmatrix} \overline{uw} \\ \overline{vw} \end{bmatrix} = qlS_M \frac{\partial}{\partial z}\begin{bmatrix} U \\ V \end{bmatrix} \quad (22)$$

$$-\overline{w\theta} = qlS_H \frac{\partial \Theta}{\partial z}, \quad (23)$$

where the nondimensional vertical exchange coefficients, S_M and S_H, are given by Galperin et al. (1988). The presence of the Coriolis terms, however, substantially complicates these equations. In addition, rotation introduces asymmetry in Eqs. (16)–(19), thus imparting vertical exchange coefficients with tensorial properties.

For further analysis let us define the following dimensionless variables:

$$Ru \equiv \frac{l}{q}\frac{\partial U}{\partial z}, \quad Rv \equiv \frac{l}{q}\frac{\partial V}{\partial z}; \quad (24a,b)$$

$$\mathrm{Ro}_y^{-1} \equiv \frac{l}{q} f_y, \quad \mathrm{Ro}_z^{-1} \equiv \frac{l}{q} f; \quad (25a,b)$$

$$G_H \equiv -\left(\frac{l}{q}\right)^2 \beta g \frac{\partial \Theta}{\partial z}; \tag{26}$$

$$\widetilde{\overline{u_i u_j}} = \frac{\overline{u_i u_j}}{q^2}, \quad \overline{u_i \theta} = \frac{l \beta g \widetilde{\overline{u_i \theta}}}{q^3}. \tag{27a,b}$$

Substituting Eqs. (24)–(27) in (16)–(19), one obtains the following matrix equation:

$$\mathbf{AX} = \mathbf{B}, \tag{28}$$

where

$$\mathbf{A} = \mathbf{A}_0 + \mathrm{Ro}_y^{-1}\mathbf{A}_y + \mathrm{Ro}_z^{-1}\mathbf{A}_z, \tag{29}$$

and

$$\mathbf{A}_0 = \begin{bmatrix} 1 & 3A_1Rv & 3A_1Ru & 0 & 0 & 0 & 0 & 0 & 0 \\ 0 & 1 & 0 & -3A_1 & 0 & 0 & 0 & 0 & 3A_1Ru \\ 0 & 0 & 1 & 0 & -3A_1 & 0 & 0 & 0 & 3A_1Rv \\ 0 & -3A_2G_H & 0 & 1 & 0 & 3A_2Ru & 0 & 0 & 0 \\ 0 & 0 & -3A_2G_H & 0 & 1 & 3A_2Rv & 0 & 0 & 0 \\ 0 & 0 & 0 & 0 & 0 & (1 - 3A_2B_2G_H) & 0 & 0 & -3A_2G_H \\ 0 & 6A_1Ru & 0 & 0 & 0 & 0 & 1 & 0 & 0 \\ 0 & 0 & 6A_1Rv & 0 & 0 & 0 & 0 & 1 & 0 \\ 0 & 0 & 0 & 0 & 0 & -6A_1 & 0 & 0 & 1 \end{bmatrix}, \tag{30}$$

$$\mathbf{A}_y = \begin{bmatrix} 0 & 0 & 3A_1 & 0 & 0 & 0 & 0 & 0 & 0 \\ 0 & 0 & 0 & 0 & 0 & 0 & -3A_1 & 0 & 3A_1 \\ -3A_1 & 0 & 0 & 0 & 0 & 0 & 0 & 0 & 0 \\ 0 & 0 & 0 & 0 & 0 & 3A_2 & 0 & 0 & 0 \\ 0 & 0 & 0 & 0 & 0 & 0 & 0 & 0 & 0 \\ 0 & 0 & 0 & -3A_2 & 0 & 0 & 0 & 0 & 0 \\ 0 & 6A_1 & 0 & 0 & 0 & 0 & 0 & 0 & 0 \\ 0 & 0 & 0 & 0 & 0 & 0 & 0 & 0 & 0 \\ 0 & -6A_1 & 0 & 0 & 0 & 0 & 0 & 0 & 0 \end{bmatrix}, \tag{31}$$

$$\mathbf{A}_z = \begin{bmatrix} 0 & 0 & 0 & 0 & 0 & 0 & 3A_1 & -3A_1 & 0 \\ 0 & 0 & -3A_1 & 0 & 0 & 0 & 0 & 0 & 0 \\ 0 & 3A_1 & 0 & 0 & 0 & 0 & 0 & 0 & 0 \\ 0 & 0 & 0 & 0 & -3A_2 & 0 & 0 & 0 & 0 \\ 0 & 0 & 0 & 3A_2 & 0 & 0 & 0 & 0 & 0 \\ 0 & 0 & 0 & 0 & 0 & 0 & 0 & 0 & 0 \\ -6A_1 & 0 & 0 & 0 & 0 & 0 & 0 & 0 & 0 \\ 6A_1 & 0 & 0 & 0 & 0 & 0 & 0 & 0 & 0 \\ 0 & 0 & 0 & 0 & 0 & 0 & 0 & 0 & 0 \end{bmatrix}, \tag{32}$$

$$\mathbf{X} = \begin{bmatrix} \overline{uv} \\ \overline{uw} \\ \overline{vw} \\ \overline{u\theta} \\ \overline{v\theta} \\ \overline{w\theta} \\ \overline{u^2} \\ \overline{v^2} \\ \overline{w^2} \end{bmatrix}, \quad \mathbf{B} = \begin{bmatrix} 0 \\ 3A_1C_1Ru \\ 3A_1C_1Rv \\ 0 \\ 0 \\ 0 \\ \frac{1}{3}\left(1 - \frac{6A_1}{B_1}\right) \\ \frac{1}{3}\left(1 - \frac{6A_1}{B_1}\right) \\ \frac{1}{3}\left(1 - \frac{6A_1}{B_1}\right) \end{bmatrix}. \tag{33), (34}$$

Tilde overbars over $\overline{u_iu_j}$ and $\overline{u_i\theta}$ are omitted in Eq. (33). The formal solution to Eq. (28) is given by

$$\mathbf{X} = \mathbf{A}^{-1}\mathbf{B}. \tag{35}$$

When Ro_y^{-1} and Ro_z^{-1} are set to zero in Eq. (28) the level 2½ model version of Galperin et al. (1988) is recovered. Manipulation of the set of Eqs. (16)–(19) reduces it to the system of three, rather complex, coupled equations for $-\overline{uw}$, $-\overline{vw}$ and $-\overline{w\theta}$ which may then be solved numerically, using Kramer's rule, to relate them to the mean field gradients:

$$-\overline{uw}\left\{1 + 36A_1^2\,\mathrm{Ro}_y^{-1}(Ru + \mathrm{Ro}_y^{-1}) - 9A_1A_2G_H + \frac{81A_1A_2^3\,\mathrm{Ro}_z^{-2}G_H}{1 + 9A_2^2\,\mathrm{Ro}_z^{-2}} + \frac{54A_1^3\,\mathrm{Ro}_y^{-1}\,\mathrm{Ro}_z^{-1}}{1 + 36A_1^2\,\mathrm{Ro}_z^{-2}}\right.$$
$$\left.\times\,[Rv - 6A_1\,\mathrm{Ro}_z^{-1}(Ru + \mathrm{Ro}_y^{-1})]\right\} - \overline{vw}\left[-3A_1\,\mathrm{Ro}_z^{-1} - \frac{27A_1A_2^2\,\mathrm{Ro}_z^{-1}G_H}{1 + 9A_2^2\,\mathrm{Ro}_z^{-2}} + \frac{54A_1^3\,\mathrm{Ro}_y^{-1}\,\mathrm{Ro}_z^{-1}}{1 + 36A_1^2\,\mathrm{Ro}_z^{-2}}\right.$$
$$\left.\times\,(Ru + \mathrm{Ro}_y^{-1} + 6A_1\,\mathrm{Ro}_z^{-1}Rv)\right] - \overline{w\theta}\left\{18A_1^2Ru + 9A_1A_2(Ru + \mathrm{Ro}_y^{-1}) + \frac{27A_1A_2^2\,\mathrm{Ro}_z^{-1}}{1 + 9A_2^2\,\mathrm{Ro}_z^{-2}}\right.$$
$$\left.\times\,[Rv - 3A_2\,\mathrm{Ro}_z^{-1}(Ru + \mathrm{Ro}_y^{-1})] + 18A_1^2\,\mathrm{Ro}_y^{-1}\right\} = A_1\left(1 - \frac{6A_1}{B_1} - 3C_1\right)Ru = B_1^{-1/3}Ru, \tag{36}$$

$$-\overline{uw}\left\{18A_1^2\,\mathrm{Ro}_y^{-1}Rv + 3A_1\,\mathrm{Ro}_z^{-1} + \frac{27A_1A_2^2\,\mathrm{Ro}_z^{-1}G_H}{1 + 9A_2^2\,\mathrm{Ro}_z^{-2}} + \frac{9A_1^2\,\mathrm{Ro}_y^{-1}}{1 + 36A_1^2\,\mathrm{Ro}_z^{-2}}\right.$$
$$\left.\times\,[Rv - 6A_1\,\mathrm{Ro}_z^{-1}(Ru + \mathrm{Ro}_y^{-1})]\right\} - \overline{vw}\left[1 - \frac{9A_1A_2G_H}{1 + 9A_2^2\,\mathrm{Ro}_z^{-2}} + \frac{9A_1^2\,\mathrm{Ro}_y^{-1}}{1 + 36A_1^2\,\mathrm{Ro}_z^{-2}}\right.$$
$$\left.\times\,[Ru + \mathrm{Ro}_y^{-1} + 6A_1\,\mathrm{Ro}_z^{-1}Rv)\right] - \overline{w\theta}\left\{18A_1^2Rv + \frac{9A_1A_2}{1 + 9A_2^2\,\mathrm{Ro}_z^{-2}}\right.$$
$$\left.\times\,[Rv - 3A_2\,\mathrm{Ro}_z^{-1}(Ru + \mathrm{Ro}_y^{-1})]\right\} = A_1\left(1 - \frac{6A_1}{B_1} - 3C_1\right)Rv = B_1^{-1/3}Rv, \tag{37}$$

$$-\overline{uw}\left[18A_1A_2\,\mathrm{Ro}_y^{-1} + 9A_2^2\,\mathrm{Ro}_y^{-1} - \frac{81A_2^4\,\mathrm{Ro}_y^{-1}\,\mathrm{Ro}_z^{-2}}{1 + 9A_2^2\,\mathrm{Ro}_z^{-2}}\right] - \overline{vw}\left[\frac{27A_2^3\,\mathrm{Ro}_y^{-1}\,\mathrm{Ro}_z^{-1}}{1 + 9A_2^2\,\mathrm{Ro}_z^{-2}}\right]$$
$$+ \frac{\overline{w\theta}}{G_H}\left\{1 - 18A_1A_2G_H - 3A_2B_2G_H + 9A_2^2\,\mathrm{Ro}_y^{-1}(Ru + \mathrm{Ro}_y^{-1})\right.$$
$$\left. + \frac{27A_2^3\,\mathrm{Ro}_y^{-1}\,\mathrm{Ro}_z^{-1}}{1 + 9A_2^2\,\mathrm{Ro}_z^{-2}}[Rv - 3A_2\,\mathrm{Ro}_z^{-1}(Ru + \mathrm{Ro}_y^{-1})]\right\} = A_2\left(1 - \frac{6A_1}{B_1}\right). \tag{38}$$

An alternative approach is to use the symbolic computer language, REDUCE, to solve the set of equations (16)–(19) symbolically. We have used both methods to deal with the above set of equations. This approach allowed us to double check the algebra and to reveal some interesting details that might otherwise have been overlooked.

We wish now to analyze Eq. (35) and obtain some preliminary estimates of the impact of rotation on the Reynolds stresses and heat fluxes. Thus, we write

$$\mathbf{X} = \mathbf{A}^{-1}\mathbf{B} = (\mathbf{A}_0 + \mathrm{Ro}_y^{-1}\mathbf{A}_y + \mathrm{Ro}_z^{-1}\mathbf{A}_z)^{-1}\mathbf{B}$$
$$= [\mathbf{A}_0(\mathbf{I} + \mathrm{Ro}_y^{-1}\mathbf{V}\mathbf{A}_y + \mathrm{Ro}_z^{-1}\mathbf{V}\mathbf{A}_z)]^{-1}\mathbf{B}$$
$$= (\mathbf{I} + \mathrm{Ro}_y^{-1}\mathbf{V}\mathbf{A}_y + \mathrm{Ro}_z^{-1}\mathbf{V}\mathbf{A}_z)^{-1}\mathbf{V}\mathbf{B}, \tag{39}$$

where

$$\mathbf{V} \equiv \mathbf{A}_0^{-1}, \tag{40}$$

and $\mathbf{I}$ is the unit matrix. The effect of rotation on the turbulence correlations, Eq. (33), is measured, therefore, by the relative importance of the matrices, $\mathrm{Ro}_y^{-1}\mathbf{V}\mathbf{A}_y$ and $\mathrm{Ro}_z^{-1}\mathbf{V}\mathbf{A}_z$, compared to $\mathbf{I}$. A convenient way to compare matrices is to think of them as of linear operators and to compare their norms. In appendix B an appropriate analysis is given showing that in the likely range of variation of G_H, the norm, $\|\mathbf{V}\mathbf{A}_y\|$, varies between 10 and 100 and the norm, $\|\mathbf{V}\mathbf{A}_z\|$, varies between 10 and 30. Both norms are closer to their lower bounds for stable stratification indicating that stable stratification tends to reduce the effects of rotation. Appendix B also provides an approximation to Eq. (39) valid for small rotational effects.

In the case of stable stratification the constraint (12) yields the following estimations of the inverse Rossby numbers:

$$\mathrm{Ro}_y^{-1} \equiv \frac{f_y l}{q} \leqslant 0.53 \frac{f_y}{N},$$

$$|\mathrm{Ro}_z^{-1}| \equiv \frac{|f| l}{q} \leqslant 0.53 \frac{|f|}{N}.$$

Taking f_y, $|f| \approx 10^{-4}\,\mathrm{s}^{-1}$, and $N \approx 10^{-2}\,\mathrm{s}^{-1}$, which is typical for the thermocline, one finds

$$\mathrm{Ro}_y^{-1},\ |\mathrm{Ro}_z^{-1}| \leqslant 0.005.$$

As was shown in appendix B, both $\|\mathbf{VA}_y\|$ and $\|\mathbf{VA}_z\|$ do not exceed 20 for strong stable stratification; therefore, the total contribution of the rotational terms is limited according to

$$|\mathrm{Ro}_y^{-1}|\,\|\mathbf{VA}_y\|,\quad |\mathrm{Ro}_z^{-1}|\,\|\mathbf{VA}_z\| \leqslant 0.1. \quad (41)$$

Since the norms analysis provides an upper bound of the effects of rotation, their actual influence on the vertical fluxes might be smaller. Therefore, rotational effects on turbulence appear to be not overly important near the thermocline. On the other hand, there might be a stronger impact of rotation on neutral and unstable flows where matrix norms are bigger and also inverse Rossby numbers are unbounded; indeed, the effect of rotation is thought to be important in turbomachinery (Lakshminarayana 1986). Appendix A describes possibly significant modifications of the mean and turbulence structures caused by the Coriolis terms in neutral flows.

5. Effects of rotation in the constant flux layer

The dynamics of turbulence in geophysical boundary layers are usually controlled by the momentum and heat fluxes at the surface. It is useful therefore to analyze the general set of equations obtained in the previous section applied to the surface layer where these fluxes are approximately constant with height, i.e., in the constant flux layer. After some exploratory analysis, it turns out that we can form generalized Monin–Obukhov variables:

$$\frac{\kappa z}{u_\tau}\frac{\partial U}{\partial z} = (\cos\alpha\Phi_{MUU} + \sin\alpha\Phi_{MUV}), \quad (42)$$

$$\frac{\kappa z}{u_\tau}\frac{\partial V}{\partial z} = (\cos\alpha\Phi_{MVU} + \sin\alpha\Phi_{MVV}), \quad (43)$$

$$\frac{\kappa z u_\tau}{H}\frac{\partial \Theta}{\partial z} = \Phi_H, \quad (44)$$

where Φ_{MUU}, Φ_{MUV}, Φ_{MVU}, Φ_{MVV} and Φ_H are stability functions of ζ, ζ_y and ζ_z defined according to

$$\zeta \equiv \frac{z}{L},\quad \zeta_y \equiv \frac{z}{L_y},\quad \zeta_z \equiv \frac{z}{L_z}, \quad (45a,b,c)$$

where

$$L \equiv \frac{u_\tau^3}{\kappa\beta g H},\quad L_y \equiv \frac{u_\tau}{\kappa f_y},\quad L_z \equiv \frac{u_\tau}{\kappa f} \quad (46a,b,c)$$

are Monin–Obukhov length scale and rotational length scales, respectively; u_τ is the friction velocity defined by $u_\tau^2 = \tau/\rho_0$; τ is the surface shear stress; $\boldsymbol{\tau} = \tau(\cos\alpha, \sin\alpha)$; $H = (-\overline{w\theta})_0$ is the kinematic surface heat flux, and the assumption $l = \kappa z$ has been made. Equations (42) to (45) can be related to Eqs. (36), (37) and (38) according to

$$\frac{\kappa z}{u_\tau}\frac{\partial U}{\partial z} = \frac{q}{u_\tau}Ru,\quad \frac{\kappa z}{u_\tau}\frac{\partial V}{\partial z} = \frac{q}{u_\tau}Rv,$$

$$\frac{\kappa z u_\tau}{H}\frac{\partial \Theta}{\partial z} = -\left(\frac{q}{u_\tau}\right)^2 \frac{G_H}{\zeta}.$$

Generally, constant flux layers are in local equilibrium so that tendency and diffusion terms can be dropped in the energy equation thus making it algebraic and reducing the turbulence closure scheme to the level 2 model (Mellor and Yamada 1982). The nondimensionalized Eq. (6) will read in this case:

$$-\overline{uw}Ru - \overline{vw}Rv + \overline{w\theta} = B_1^{-1}. \quad (47)^1$$

The stability functions defined by Eqs. (42)–(44) should satisfy Eq. (47) as well.

In the general case of arbitrary rotation and stratification, the expressions for Φ_{MUU}, Φ_{MUV}, Φ_{MVU}, Φ_{MVV} and Φ_H are complicated and are studied separately (Kantha et al. 1989). Here, we shall simply evaluate the combined effects of rotation and stratification on the constant flux layer presenting the result of a first-order expansion in ζ, ζ_y and ζ_z. Thus,

$$\Phi_{MUU} = \Phi_{MVV} = 1 + \beta_{uuy}\zeta_y + \beta_{uuh}\zeta, \quad (48)$$

$$\Phi_{MUV} = -\Phi_{MVU} = \beta_{uvz}\zeta_z, \quad (49)$$

$$\Phi_H = \mathrm{Pr}_t + \beta_{hy}\zeta_y + \beta_h\zeta, \quad (50)$$

which recognizes that $\beta_{uuz} = \beta_{uvy} = \beta_{uvh} = \beta_{hz} = 0$. Furthermore, we find that

$$\beta_{uuy} = 27A_1^2 B_1^{-2/3}\cos\alpha = 3.51\cos\alpha, \quad (51)$$

---

[1] Taken in the matrix form, Eq. (47) adds a row to the matrix $\mathbf{A}_0$, Eq. (30):

$$(0\quad -Ru\quad -Rv\quad 0\quad 0\quad 1\quad 0\quad 0\quad 0).$$

Corresponding zero rows should also be added to the matrices $\mathbf{A}_y$ and $\mathbf{A}_z$, Eqs. (31) and (32). The column, **B**, Eq. (34), should be supplemented by a term, B_1^{-1}. As a result, a system of 10 linear algebraic equations with 9 unknown variables is obtained. It can be shown, using a linear algebra theorem (sometimes referred to as the Kronecker–Capelli theorem), that the latter system of equations has a nontrivial solution if and only if the augmented matrix of this system has a zero determinant. (The augmented matrix is obtained by adding the column, **B**, to the original 10×9 matrix). This requirement merely guarantees that not all of the 10 equations are linearly independent, and therefore the system is not overdetermined. The resulting equation defines a surface on which all possible values of the independent variables can lie. For neutral nonrotating flows, this requirement provides $Ru^2 + Rv^2 = B_1^{-2/3}$, which means that all possible values of Ru and Rv belong on the circle with the radius $B_1^{-1/3}$. In a general case of rotating stratified flow, this surface may have quite a complicated structure.

$$\beta_{uuh} = \frac{3}{4}\left\{\frac{1}{3} + 9A_1B_1^{-2/3}[2A_1 + (1 + \mathrm{Pr}_t)A_2]\right\} = 3.27, \quad (52)$$

$$\beta_{uvz} = -3A_1B_1^{-1/3} = -1.08, \quad (53)$$

$$\beta_{hy} = 9B_1^{-2/3}\,\mathrm{Pr}_t \cos\alpha[A_1(2A_2\,\mathrm{Pr}_t - A_1) + A_2^2(1 + \mathrm{Pr}_t)] = 1.34\cos\alpha, \quad (54)$$

$$\beta_h = \mathrm{Pr}_t\left\{3B_1^{-2/3}\left[A_2\,\mathrm{Pr}_t(6A_1 + B_2) - \frac{3}{4}A_1[2A_1 + A_2(1 + \mathrm{Pr}_t)]\right] + \frac{1}{4}\right\} = 2.76, \quad (55)$$

and where the turbulent Prandtl number, Pr_t, is given by

$$\mathrm{Pr}_t = B_1^{-1/3}/[A_2(1 - 6A_1/B_1)] = 0.79 \quad (56)$$

(Mellor and Yamada 1982).

Several interesting conclusions can be drawn from Eqs. (48)–(56):

1) The functions, Φ_{MUV} and Φ_{MVU}, describing the intercomponent momentum exchange due to f, are excluded in those closure models that neglect Coriolis terms in the turbulence equations.

2) The effects of the poleward component of the Coriolis parameter, f_y, depend on the direction of the surface stress since β_{uuy} and β_{hy} include the factor, $\cos\alpha$. In the coordinate system generally used in oceanic models, with axis x directed eastward, axis y—poleward and axis z upward, β_{uuy} and β_{hy} are positive and maximal for westerly winds, negative and minimal for easterlies and zero for meridional winds. Therefore, f_y acts to stabilize mean flows driven by westerlies and to destabilize flows caused by easterlies. This conclusion agrees with that by Garwood et al. (1985b). However, the extended analysis performed in appendix A for neutral flows demonstrates that increasing destabilization gives way to restabilization and total suppression of turbulence.

To evaluate profiles of mean velocity and temperature, Eqs. (42)–(44) can be integrated, using Eqs. (48)–(56), resulting in log-linear profiles:

$$\frac{U(z)}{u_\tau} = \frac{1}{\kappa}\left\{\cos\alpha \ln\left(\frac{z}{z_0}\right) + [(\gamma_y\beta_{uuy} + \beta_{uuh})\cos\alpha + \gamma_z\beta_{uvz}\sin\alpha]\zeta\right\}, \quad (57)$$

$$\frac{V(z)}{u_\tau} = \frac{1}{\kappa}\left\{\sin\alpha \ln\left(\frac{z}{z_0}\right) + [\gamma_z\beta_{vuz}\cos\alpha + (\gamma_y\beta_{vvy} + \beta_{vvh})\sin\alpha]\zeta\right\}, \quad (58)$$

$$\frac{\Theta - \Theta_0}{H/u_\tau} = \frac{1}{\kappa}\left[\mathrm{Pr}_t \ln\left(\frac{z}{z_T}\right) + (\gamma_y\beta_{hy} + \beta_h)\zeta\right], \quad (59)$$

where z_0 and z_T are momentum and temperature roughness parameters, and

$$\gamma_y \equiv \frac{\zeta_y}{\zeta} = \frac{L}{L_y} = \frac{u_\tau^2 f_y}{\beta g H} \quad (60a)$$

$$\gamma_z \equiv \frac{\zeta_z}{\zeta} = \frac{L}{L_z} = \frac{u_\tau^2 f}{\beta g H} \quad (61a)$$

are constants defined for a given flow by external parameters only. Obviously, rotation can enhance or relax the effects of stratification. Furthermore, for any given α, f_y and f, values of γ_y and γ_z exist such that the effects of rotation and stratification cancel each other in one of the mean profiles.

To appreciate the effects of rotation on atmospheric and oceanic mixed layers, it will be convenient to express γ_y and γ_z in terms of surface stress and heat flux which are continuous at the interface:

$$\gamma_y = \frac{c_p f_y \tau}{\beta g Q}; \quad (60b)$$

$$\gamma_z = \frac{c_p f \tau}{\beta g Q}, \quad (61b)$$

where $Q = c_p\rho_0 H$ is a heat flux. Taking f_y, $f \approx 10^{-4}$ s^{-1}, $g \approx 10$ m s^{-2}, $\tau \approx 0.05$ N m^{-2}, and $|Q| \approx 50$ W m^{-2}, one finds for the atmosphere ($c_p \approx 10^3$ J kg^{-1} K^{-1}, $\beta \approx 3.5 \times 10^{-3}$ K^{-1})

$$|\gamma_y|, |\gamma_z| \approx 0.003 \quad (62)$$

and for the ocean ($c_p \approx 4.2 \times 10^3$ J kg^{-1} K^{-1}, $\beta \approx 2 \times 10^{-4}$ K^{-1})

$$|\gamma_y|, |\gamma_z| \approx 0.21. \quad (63)$$

One can see that the effect of rotation on oceanic mixed layers is relatively weak and two orders of magnitude weaker on the atmospheric mixed layers. Analysis provided in appendix A suggests that the effect of rotation on the constant flux sublayer of neutral boundary layers is also small.

In the special case of neutral flow where $f = 0$ and $\alpha = 0$, but where $f_y \neq 0$ (known in engineering applications as spanwise rotation), Eq. (57) provides

$$\frac{U(z)}{u_\tau} = \frac{1}{\kappa}\left[\ln\left(\frac{z}{z_0}\right) + \beta_{uuy}\zeta_y\right]. \quad (64)$$

The value of $\beta_{uuy} = 3.51$, given by Eq. (51), compares well with estimates by Watmuff et al. (1985) of $\beta_{uuy} = 3$ to 5 for destabilizing rotation and $\beta_{uuy} = 2$ to 4 for stabilizing rotation and by Koyama et al. (1979) where $\beta_{uuy} = 1$ to 4. By fitting Halleen and Johnston's (1967) experimental results, Bradshaw (1969) has found that β_{uuy} is about 4 for stabilizing and 2 for destabilizing rotation.

A more thorough study of the rotational effects on neutral flows is given by Galperin and Kantha (1989). That work also includes comparisons with other closure models in use in engineering applications. Some results

of this study are summarized in appendix A, in which geophysical aspects of the problem are particularly emphasized.

Summarizing, the results of this section provide an extension of similar analyses by Monin and Yaglom (1971, Chapt. 4) and by Mellor (1973) which were restricted to the case of density stratification.

6. Modeling oceanic mixed layers

From appendix A it is clear that the effects of rotation on turbulence are important in many cases, especially in flows in turbomachinery, which are characterized by high rotation rates and the absence of stratification effects due to gravity. However, it is not clear a priori whether the rotational effects are important or not, in oceanic flows. It had generally been assumed, with little justification, that rotational terms can be ignored in oceanic turbulence. Recently Garwood et al. (1985a) have raised doubts about this assumption. These authors suggest that turbulence terms proportional to f_y, the rotational terms, could account for the difference in the depths of the mixed layers in the eastern and western parts of the equatorial Pacific Ocean. This hypothesis is appealing and Price et al. (1987) characterize it as "the most provocative new theory for mixed layer models." Among the deficiencies of this approach are the exclusive use of turbulence energetic considerations without reference to the mean momentum balance, and the introduction of their assumptions with regard to the relevant length scale. Still it is a plausible hypothesis, a hypothesis, however, that can be readily tested by the turbulence model developed in the earlier sections. In this section, we shall detail the experiments that were undertaken to do so. For this purpose, a one-dimensional version of the closure model was used to simulate the dynamics and thermodynamics of the upper ocean as an initial value problem; all properties are stipulated to be horizontally homogeneous. Generally, mixed layer models of this kind are thought to perform reasonably well at midlatitudes (Martin 1985[2]); they have been routinely incorporated in various atmospheric and oceanic circulation models (Rosati and Miyakoda 1988; Miyakoda and Sirutis 1977) and used in operational models (Clancy et al. 1988). Specifically, various versions of the present model have been shown to account for the effects of stratification and other extra strains and to produce realistic values of critical Richardson numbers at which turbulence ceases (Mellor 1973, 1975; Galperin and Kantha 1989). These results were obtained using the same set of empirical constants initially found from simulations of simple well documented flows, and therefore the level of empirism is minimized. For the present purpose, it is important to note that the rotational terms do not require any additional modeling. In a one-dimensional formulation rotational effects are not masked by other complicating factors.

To analyze the effect of rotation on the oceanic mixed layer, two series of numerical simulations were carried out. In the first series, a general appreciation of the rotational effects on stably stratified mixed layers at different latitudes and different initial and boundary conditions was sought. For this purpose, various experiments were conducted with a prescribed zonal wind stress (± 0.1 N m^{-2}) and zero meridional stress at the surface of an initially linearly stratified ocean. The stratifications used were: 0.01, 0.025, 0.05 and 0.075°C m^{-1}, which are values typical for the upper ocean. Two simulations were performed for each case, one in which the rotational terms were set to zero in the turbulence equations and the other in which they were retained. In almost all of these experiments, the mixed layer depth for zero and nonzero rotational cases differed by no more than $\mp 5\%$ at a given instant of time. Only under conditions of neutral or near neutral stratification did the experiments indicate substantial differences in the mixed layer depth (50% or so for the neutral case with rotation when compared to that without). This behavior can be traced directly to the behavior of the turbulence length scale which is inhibited by stable stratification, particularly at the base of the mixed layer where the stable density gradient is strong. Consequently, the effect of rotation on turbulence and indirectly on the mixed layer evolution tends to be small in the presence of ambient stable stratification. Since oceanic mixed layers are invariably capped by a stably stratified interface, these experiments indicate that rotational effects are small in the oceanic context.

In the second series of numerical experiments, particular attention was concentrated on the evaluation of the Garwood et al. hypothesis. Mixed layer development was modeled with surface wind stress and heat flux applied impulsively to a quiescent body of water. Three different latitudes (0°, 2° and 4°N) and four longitudes (which identify wind stress values) chosen by Garwood et al. (1985b) were selected as locations for conducting numerical simulations. The initial ambient temperature profiles, surface buoyancy fluxes and wind stresses for these simulations were adopted from the study by Garwood et al. (1985b) as given in their Figs. 1, 3 and 4, respectively. Thirty day simulations were performed with and without rotation. This period

[2] Martin (1985) performed calculations using the Mellor–Yamada (M–Y) models and using the bulk models of Garwood (1977) and Niiler (1975); all were compared to observations at stations Papa and November. A succinct summary is his Table 4 which tabulates the monthly average errors in surface temperatures. The maximum errors occurred in the late summer and fall. Thus, at station November the M–Y models results were too warm by 1.5°C and the Niiler and Garwood models were too cold by 0.7°; at station Papa the M–Y models were too warm by 2.2° and the Niiler and Garwood models were too cold by 3.0° and 1.8° respectively. It is important to state that, for Garwood's model, Martin chose model constants to best fit the data; furthermore, both bulk models assume the existence of a surface mixed layer a priori and the models and their constants are specific to that application. The M–Y models had fixed constants determined from laboratory turbulence data and can cope with a fairly broad range of turbulence problems.

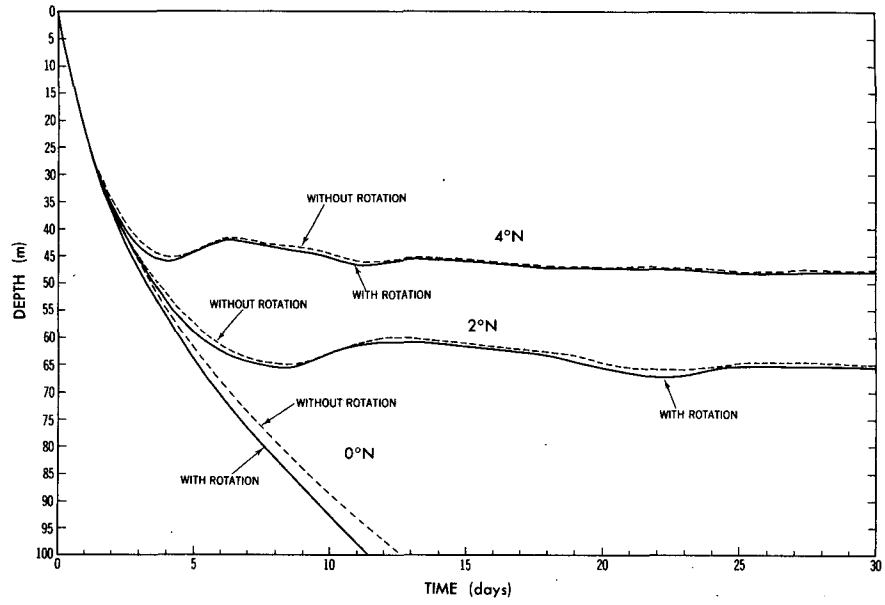

FIG. 1. Mixed layer depths with and without rotational effects on turbulence at 0°, 2° and 4°N latitudes. Longitude 160°W, heat flux 23.1 W m^{-2}, $\tau_x/\rho = 0.49 \times 10^{-4}$ m^2 s^{-2}, $\tau_y/\rho = 0.05 \times 10^{-4}$ m^2 s^{-2}.

encompasses at least two full cycles of inertial oscillations during which the mixed layer depth (MLD) attained a quasi-steady value (inertial period at 2°N is about 14 days). As has been emphasized in the Introduction, a simulation of the equatorial mixed layer yields a continuously deepening mixed layer; one needs advection and/or pressure gradient terms to obtain a steady state.

In all the simulations performed in the second series, only a mild effect of rotation on MLD was found, within 10%. As expected from the theory, the mixed layer was deeper for easterly winds and shallower for westerlies (since the results for westerlies are quantitatively similar to easterlies, they are not shown here). These tendencies are similar to those of Garwood et al. (1985b) but the influence of rotation is substantially less. Figure 1 compares an evolution of MLD with and without the effect of rotation for three latitudes, 0°, 2° and 4°N, and for the longitude 160°W (only the results for these particular locations are shown here. Other runs provided similar results.). One can see that in both cases the MLD oscillates with inertial frequency and with decreasing amplitude and tends to reach a steady state. Figure 2 compares vertical profiles of zonal and meridional velocities, U and V, at 2°N (the results for 4°N are qualitatively similar and, therefore, not shown). Notice a small difference between the profiles in the bulk of the mixed layer which disappears towards the bottom of the layer, where effects of rotation are limited by ambient stratification. Vertical profiles in the case with rotation are slightly flatter but the differences between the two cases are, again, well below 10%. The flattening of the velocity profiles and consequent decrease in the production of turbulence energy are probably behind the decrease in turbulence energy in rotational case as shown in Fig. 3. Nevertheless, in this case, too, the differences between rotational and non-rotational cases barely reach 10%. Recall again that limited effect of rotation on oceanic mixed layers is related to the influence of stable stratification in limiting the turbulence macroscale, l, as dictated by the constraint (12). Thus, for stably stratified flows, the effect of rotation, at least in the geophysical context, appears to be rather small, a conclusion that differs from that of Garwood et al.

The Garwood et al. (1985b) analysis of the equatorial mixed layer is based on a vertically integrated one-dimensional model of the turbulence energetics in

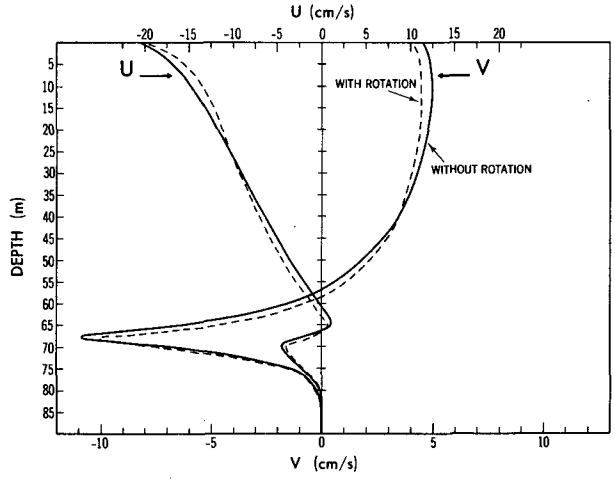

FIG. 2. As in Fig. 1 but mean velocity profiles with and without rotational effects on turbulence.

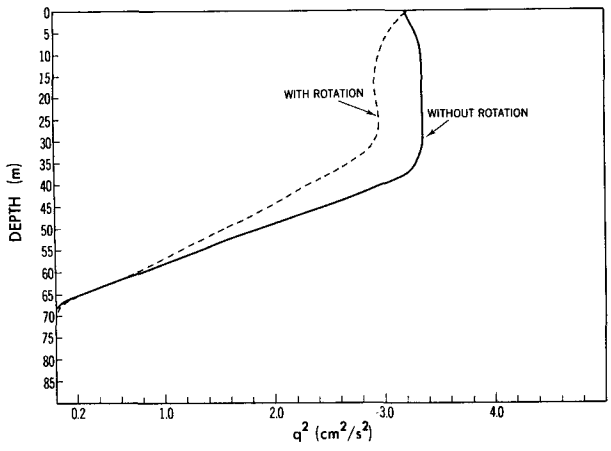

FIG. 3. As Fig. 1 but turbulence kinetic energy profiles with and without rotational effects on turbulence.

the presence of rotational terms, a direct extension of earlier Garwood mixed layer model for higher latitudes (Garwood 1977, 1979). Thus the resulting expression for MLD is similar to that for higher latitudes except that the Ekman length scale, $L_E \equiv u_\tau/f$, is replaced by L_y in the expression, leading to

$$\text{MLD} \propto 1/(L^{-1} + L_y{}^{-1})$$

for equatorial regions. At the equator this yields a finite MLD; however the mean momentum equation does not possess a steady state if $L_E \to \infty$ (see Fig. 1) and the flow is horizontally homogeneous.

7. Concluding remarks

This study demonstrates that rotational effects are sensitive to local flow characteristics including the local turbulence structure. It is for this reason that stable stratification tends to suppress rotational effects, through its influence on the local turbulence macroscale. Other generalizations can also be made. For example, rotation imparts the eddy viscosity with tensorial properties. Nonzero f_y makes diagonal terms of this tensor unequal, whereas f causes off-diagonal terms to be nonzero. The general tendency is for nonzero f to reduce the turbulence intensity. The effect of f_y can however be both stabilizing or destabilizing, leading to a decrease or increase of mixing, respectively. However, sufficiently strong "destabilizing" f_y can decrease and eventually suppress turbulent mixing in neutral flows (see appendix A). Also, momentum considerations play an important role in mixed layer evolution, and, therefore, we believe that models that ignore this do not adequately represent the mixed layer physics. Energy considerations are but only a part of the story.

In the presence of significant stratification as in oceanic boundary layers, rotational effects are inhibited by stable stratification. Since geophysical mixed layers are invariably capped by stably stratified regions, rotational effects tend to be small overall. However, there can be non-negligible changes in the internal structure of these layers.

It is possible to establish Monin-Obukhov type similarity laws for rotational effects, with the rotational length scales, L_y and L_z, taking the place of the Monin-Obukhov scale for stratification.

The model presented here offers a self-consistent framework for studying complex turbulent flows that result when both rotational and stratification effects are included. It should therefore be of potential use in both geophysical and engineering applications.

Finally, one of the main emphases of this paper has been oceanic mixed layer evolution under zero or a stable buoyancy flux. The numerical simulations reported in the section 6 do not support the conclusions reached by Garwood et al. (1985b), as they do not reveal a dramatic effect of rotation on the depth of the mixed layer, due to stable stratification typical of the equatorial Pacific. Fernando (1987) commenting on Garwood et al. hypothesis has also questioned the importance of the rotational effects for the mixed layer turbulence. However, under a destabilizing buoyancy flux, such as that which occurs during winter cooling and diurnal cycle, the effects could be larger, although stable stratification capping the mixed layer would still tend to suppress these effects locally. Quantification of these effects is however beyond the scope of this paper.

Acknowledgments. The authors are indebted to Drs. I. Held and G. Philander for thoughtful reviews of the manuscript. Assistance of Prof. Hale Trotter, from the Department of Mathematics, Princeton University, in performing symbolic calculations using REDUCE, is greatly appreciated. BG was supported by GFDL under the NOAA Grant NA84EAD00057, by the New Jersey Commission on Science and Technology and by National Science Foundation under Grant OCE-8716027. LK wishes to acknowledge Grants ONR-N00014-84-K-O-0640 and ONR-N00014-86-C-0438. GLM was supported by the Office of Naval Research (N00014-84-K-O-0640) and the Institute for Naval Oceanography (INO-S8751-3-89). The figures were drafted by the GFDL Graphics Department and were processed by Mr. J. Conner.

APPENDIX A

Effects of Rotation on Neutral Flows

In several simple cases pertaining to neutral flows, Eqs. (16)–(19) can be solved analytically to reveal modification of the relations between Reynolds stress and mean shear in the presence of rotation. This type of flow is important in engineering applications, particularly in rotating turbomachinery, and aerodynamics (Lakshminarayana 1986). Here we shall present only a brief analysis of the effects of rotation on neutral flows; more exhaustive study is the subject of a companion paper (Galperin and Kantha 1989). Two classes of neutral flows ($G_H = 0$) will be considered when either $\text{Ro}_y{}^{-1} = 0$ or $\text{Ro}_z{}^{-1} = 0$.

a. The case when $Ro_y^{-1} = 0$

Equations (36), (37) reduce to

$$-\overline{uw} = S_{MUU}Ru + S_{MUV}Rv, \quad \text{(A1)}$$

$$-\overline{vw} = S_{MVU}Ru + S_{MVV}Rv, \quad \text{(A2)}$$

where

$$S_{MUU} = B_1^{-1/3}/(1 + 9A_1^2\,Ro_z^{-2}), \quad \text{(A3a)}$$

$$S_{MUV} = 3A_1B_1^{-1/3}\,Ro_z^{-1}/(1 + 9A_1^2\,Ro_z^{-2}), \quad \text{(A3b)}$$

$$S_{MVU} = -S_{MUV}, \quad \text{(A3c)}$$

$$S_{MVV} = S_{MUU}; \quad \text{(A3d)}$$

the matrix $\mathbf{S}_M$ is antisymmetric and its denominator is insensitive to the sign of Ro_z. Also, it does not explicitly depend on the mean shear. The presence of nonzero S_{MUV} describes intercomponent momentum exchange in the mean flow due to rotation. Increasing rotation will decrease vertical transport until turbulence is completely suppressed. Local equilibrium analysis reveals that turbulence can exist for

$$|Rr_z| \leqslant (9A_1^2B_1^{-2/3})^{-1/2} = 0.923, \quad \text{(A4)}$$

where

$$Rr_z \equiv \frac{f}{|G|}, \quad \text{(A5)}$$

$$G^2 \equiv \left(\frac{\partial U}{\partial z}\right)^2 + \left(\frac{\partial V}{\partial z}\right)^2. \quad \text{(A6)}$$

The parameter, Rr_z, can be interpreted as a rotational Richardson number, since it plays a role similar to that of the Richardson number in stratified flows.

The horizontal momentum equations for this class of flows admit a complex form with a complex eddy viscosity:

$$\frac{\partial \hat{V}}{\partial t} + if\hat{V} = \frac{\partial}{\partial z}\left(ql\hat{S}_M\frac{\partial \hat{V}}{\partial z}\right), \quad \text{(A7)}$$

where

$$\hat{S}_M = S_{MUU} - iS_{MUV}, \quad \text{(A8)}$$

$$\hat{V} = U + iV. \quad \text{(A9)}$$

b. The case when $Ro_z^{-1} = 0$

Equations (36), (37) reduce to

$$-\overline{uw} = S_{MU}Ru, \quad \text{(A10)}$$

$$-\overline{vw} = S_{MV}Rv, \quad \text{(A11)}$$

where

$$S_{MU} = B_1^{-1/3}/[1 + 36A_1^2\,Ro_y^{-1}(Ru + Ro_y^{-1})], \quad \text{(A12a)}$$

$$S_{MV} = \frac{B_1^{-1/3}[1 + 9A_1^2\,Ro_y^{-1}(Ru + 4\,Ro_y^{-1})]}{1 + 45A_1^2Ro_y^{-1}(Ru + Ro_y^{-1}) + 324A_1^4\,Ro_y^{-2}(Ru + Ro_y^{-1})^2}. \quad \text{(A12b)}$$

As Eqs. (A12a,b) indicate, the vertical exchange coefficients, S_{MU} and S_{MV}, depend explicitly on the mean zonal shear, Ru. Let us consider the cases of a purely zonal flow, in which $Rv = 0$. It will be useful for the following discussion to re-write equations for $\overline{u^2}$, $\overline{w^2}$ and $\overline{uw}$ obtained using Eqs. (16), (18), (24), (25) and (27):

$$\overline{u^2} = \frac{1}{3}\left(1 - \frac{6A_1}{B_1}\right) - 6A_1\overline{uw}Ru - 6A_1\,Ro_y^{-1}\overline{uw}, \quad \text{(A13)}$$

$$\overline{w^2} = \frac{1}{3}\left(1 - \frac{6A_1}{B_1}\right) + 6A_1\,Ro_y^{-1}\overline{uw}, \quad \text{(A14)}$$

$$-\overline{uw} = 3A_1[\overline{w^2}(1 + Rr_y) - \overline{u^2}\,Rr_y - C_1]Ru, \quad \text{(A15)}$$

where

$$Rr_y \equiv \frac{Ro_y^{-1}}{Ru} = \frac{f_y}{\partial U/\partial z} \quad \text{(A16)}$$

is another rotational Richardson number. Equations (A10) and (A15) suggest a different form for the eddy viscosity, S_{MU}:

$$S_{MU} = 3A_1[\overline{w^2}(1 + Rr_y) - \overline{u^2}\,Rr_y - C_1]. \quad \text{(A17)}$$

Equations (A13)–(A15) show that $\overline{uw}$ not only redistributes energy between $\overline{u^2}$ and $\overline{w^2}$, as was noted by Garwood et al. (1985a), but, in turn, $\overline{u^2}$ and $\overline{w^2}$ feed back on $\overline{uw}$, the effect missing in Garwood et al. (1985a) since they retained Coriolis terms in the equations for the components of turbulence energy only. This feed-back is an important component of the effect of rotation but has not been given enough attention (a brief discussion of the issue can be found in Hunt and Joubert 1979). To make the analysis simpler, we shall invoke the approximation of local equilibrium:

$$-\overline{uw}Ru = 1/B_1. \quad \text{(A18)}$$

This approach is similar to the one used by Mellor (1975) who studied the effect of streamline curvature on turbulence and So (1975) who also included the effect of spanwise rotation.

It can be shown that S_{MU} takes the form

$$S_{MU} = B_1^{-1/3}[1 - 36A_1^2B_1^{-2/3}\,Rr_y(1 + Rr_y)]. \quad \text{(A19)}$$

This expression is similar to that derived by So (1975). S_{MU} is non-negative if

$$-1.18 \leqslant Rr_y \leqslant 0.18, \quad \text{(A20)}$$

which establishes the criterion of existence of turbulence for the case under consideration. Equations (A13) and (A14) can be rewritten as

$$\overline{u^2} = \frac{1}{3}\left(1 + \frac{12A_1}{B_1}\right) + \frac{6A_1}{B_1}Rr_y, \quad \text{(A21)}$$

$$\overline{w^2} = \frac{1}{3}\left(1 - \frac{6A_1}{B_1}\right) - \frac{6A_1}{B_1}Rr_y. \quad \text{(A22)}$$

One can see that as Rr_y varies in the range given by inequalities (A20), both $\overline{u^2}$ and $\overline{w^2}$ vary in the range [0.163, 0.615], with $\overline{u^2}$ increasing and $\overline{w^2}$ decreasing with increasing Rr_y. For positive Rr_y, the eddy viscosity, S_{MU}, given by Eq. (A17), decreases until it becomes zero at approximately $Rr_y = 0.18$. On the other hand, when Rr_y decreases below zero, S_{MU} will increase until Rr_y reaches the value of -0.5 at which the energy is distributed equally between $\overline{u^2}$ and $\overline{w^2}$; at this point $\overline{u^2} = \overline{w^2} = 0.389$. As Rr_y decreases further, the contributions of $\overline{u^2}$ and $\overline{w^2}$ to S_{MU} switch causing S_{MU} to decrease again until it becomes zero at approximately $Rr_y = -1.18$. This behaviour of S_{MU} is the direct result of the feed-back of $\overline{u^2}$ and $\overline{w^2}$ on $\overline{uw}$, Eq. (A15). In Fig. A1, S_{MU}, $\overline{u^2}$ and $\overline{w^2}$, given by Eqs. (A19), (A21) and (A22) are presented as functions of Rr_y. One can see that S_{MU} is symmetrical about the axis $Rr_y = -0.5$, and $\overline{u^2}$, $\overline{w^2}$ are mirror images of each other. Positive Rr_y reduces S_{MU} and is therefore stabilizing. However, negative Rr_y can be both destabilizing and stabilizing. Figure A1 shows both the stabilization and destabilization regions.

The effect of spanwise rotation has been analyzed by earlier authors in terms of a rotation Richardson number defined as $Ri = Rr_y(1 + Rr_y)$. This definition, however, provides the same value of Ri in the two different flow situations described above, characterized by two different Rr_y, one of which is positive and the other is negative, and therefore masks the effect of restabilization. On the other hand, Rr_y is a monotonic function of the flow, and it does reveal the effect of restabilization. Besides it has a more direct analogy with the stability parameter in Monin–Obukhov similarity theory, as will be shown shortly.

Consider now the case of the constant flux wall region characterized by local equilibrium. In this region, the Reynolds stress can be expressed as follows:

$$-\overline{uw} = u_\tau^2 \cos\alpha = q l S_{MU} \frac{\partial U}{\partial z}, \qquad \text{(A23)}$$

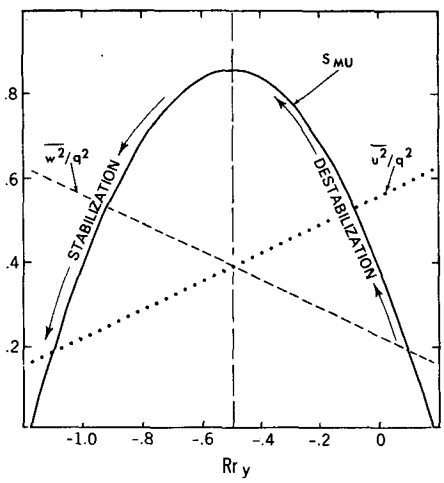

FIG. A1. Variation of nondimensional eddy viscosity and components of turbulence kinetic energy in a spanwise rotating flow.

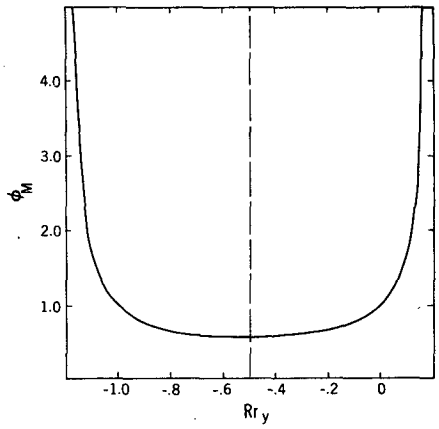

FIG. A2. Stability function, $\Phi_{MUU}(Rr_y)$, in a spanwise rotating flow.

where $\overline{uw}$ is now a dimensional variable. The local equilibrium assumption for this case is

$$-\overline{uw} \frac{\partial U}{\partial z} = u_\tau^2 \cos\alpha \frac{\partial U}{\partial z} = \frac{q^3}{B_1 l}, \qquad \text{(A24)}$$

where we assume $l = \kappa z$ near the wall. Equation (42) provides for this case

$$\frac{\partial U}{\partial z} = \frac{u_\tau}{\kappa z} \Phi_{MUU}(\zeta_y) \cos\alpha, \qquad \text{(A25)}$$

where $\alpha = 0$ for westerlies and $\alpha = \pi$ for easterlies. Substitution of Eqs. (A19), (A24) and (A25) in (A23) yields:

$$B_1^{-1/3}\Phi_{MUU}^2 - \frac{36A_1^2}{B_1}\zeta_y \Phi_{MUU} - B_1^{-1/3}\Phi_{MUU}^{2/3} - \frac{36A_1^2}{B_1}\zeta_y^2 = 0, \qquad \text{(A26)}$$

where

$$\zeta_y = \frac{z}{L_y},$$

$$L_y = \frac{u_\tau}{\kappa f_y}\cos\alpha.$$

The rotational length scale, L_y, is positive for westerlies which leads to a stabilization of the mixed layer while negative, destabilizing values of L_y are associated with easterlies. Rotational Richardson number, defined by (A16), can be written as

$$Rr_y = \frac{\zeta_y}{\Phi_{MUU}(\zeta_y)}, \qquad \text{(A27)}$$

and $\Phi_{MUU}(\zeta_y)$ as a function of Rr_y becomes

$$\Phi_{MUU}(Rr_y) = [1 - 36A_1^2 B_1^{-2/3} Rr_y(1 + Rr_y)]^{-3/4}. \qquad \text{(A28)}$$

Figure A2 shows $\Phi_{MUU}(Rr_y)$ in the range allowed by inequalities (A20). $\Phi_{MUU}(Rr_y)$ is symmetric with re-

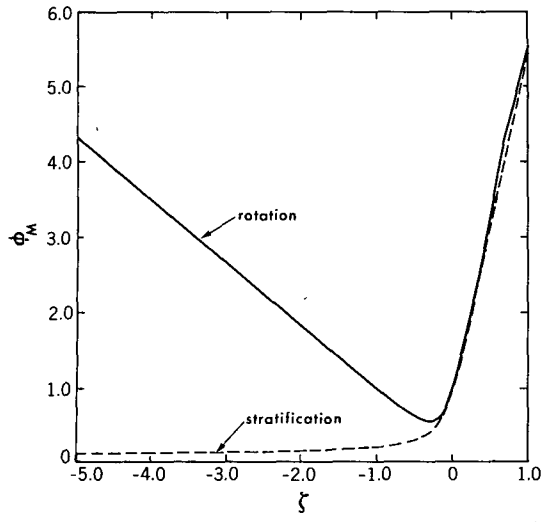

FIG. A3. Stability function, $\Phi_{MUU}(\zeta)$, in a spanwise rotating flow.

spect to the axis $\mathrm{Rr}_y = -0.5$. Figure A3 compares stability functions, $\Phi_{MUU}(\zeta_y)$ and $\Phi_M(\zeta)$, the former being calculated for a neutral rotating zonal flow and the latter—for a stratified nonrotating flow, where both stability parameters are denoted as ζ for convenience. One can see that both curves are similar for $\zeta \geqslant 0$, where flows are stabilized, and for $-0.28 \leqslant \zeta < 0$, where flows are destabilized. Under stronger destabilizing conditions, when $\zeta < -0.28$, there is a large difference between the curves, due to the effect of rotational restabilization. If large negative values of ζ, comparable with the ones typical for stratified flows, were easily attainable in geophysical situations, the effect of rotation on such flows would indeed be dramatic. The evidence of such an effect may yet be found in *rapidly rotating* systems with a relatively small rotational length scale, L_y.

An estimation of the thickness of geophysical constant flux layers with arbitrary stratification, z_p, was given by Monin and Yaglom (1971, p. 406) as $z_p \approx 0.01 u_\tau / f$, as was also obtained by Galperin and Hassid (1984); one stipulates that, in the constant flux layer, the momentum flux can change by no more than 20% of its value at the surface. Using this and the definition of L_y, Eq. (45), an estimate of ζ can be made:

$$\zeta_y \approx \frac{z_p}{L_y} = 0.01\kappa \frac{f_y}{f} = 0.01\kappa \cot\phi,$$

ϕ being the latitude. For different latitudes one will find $\zeta_y = 0.004$, 0.023, 0.046 and 0.076 for $\phi = 45°$, 10°, 5° and 3°, respectively, which indicates that the effect of rotation on constant flux layers is fairly small except in the close vicinity of the equator, $\phi \approx 3°$. At smaller latitudes, for the atmospheric boundary layer, assuming $u_\tau \approx 0.4$ m s^{-1}, $f_y \approx 10^{-4}$ s^{-1}, one finds $L_y \approx 10$ km whereas the constant flux layer is well below 1 km. This estimate is based on the data of Klebanoff (1954) for a nonrotating boundary layer over a flat plate, which roughly corresponds to the situation near the equator where $f \to 0$. According to these data, if the same criterion as before, i.e., 20% change in the surface momentum flux, is used for identification of the constant flux layer, then its thickness will reach about 30% of the boundary layer depth. Although this estimate is obtained for neutral flows, we shall assume that it can be used as an approximation for the stratified flows as well.

For the equatorial ocean, with $u_\tau \approx 0.03$ m s^{-1} and $f_y \approx 10^{-4}$ s^{-1}, we find $L_y \approx 750$ m whereas the constant flux layer barely reaches 50 m. All these estimates show that the constant flux sublayer of planetary boundary layers is only weakly affected by rotation and the absolute value of ζ_y is usually well below 0.1.

APPENDIX B

Analysis of the Matrix Equation (39)

Given an Eq. (39)

$$\mathbf{X} = (\mathbf{I} + \mathrm{Ro}_y^{-1}\mathbf{VA}_y + \mathrm{Ro}_z^{-1}\mathbf{VA}_z)^{-1}\mathbf{VB}, \quad \text{(B1)}$$

we look for conditions when this equation can be approximated as

$$\mathbf{X} \approx (\mathbf{I} - \mathrm{Ro}_y^{-1}\mathbf{VA}_y - \mathrm{Ro}_z^{-1}\mathbf{VA}_z)\mathbf{VB}. \quad \text{(B2)}$$

Thinking of matrices as of linear operators in vector space, one may recall that the first order expansion (B2) is valid if the norms of $\mathrm{Ro}_y^{-1}\mathbf{VA}_y$, $\mathrm{Ro}_z^{-1}\mathbf{VA}_z$ are much smaller than the norm of $\mathbf{I}$ (=1), or

$$|\mathrm{Ro}_y^{-1}|\,\|\mathbf{VA}_y\|, \quad |\mathrm{Ro}_z^{-1}|\,\|\mathbf{VA}_z\| \ll 1. \quad \text{(B3)}$$

Equation (B2) is substantially simpler than (B1) since it requires inversion of only one matrix, $\mathbf{A}_0$.

All the operators, $\mathbf{A}_0$, $\mathbf{A}_y$, $\mathbf{A}_z$ are continuous and, therefore, they are bounded (Kolmogorov and Fomin 1968). Also, for each of the operators a constant C_i does exist, such that

$$\|\mathbf{A}_i f\| \leqslant C_i \|f\|, \quad i = 1, 2, 3, \quad \text{or} \quad i = 0, y, z, \quad \text{(B4)}$$

where f is an arbitrary vector and $\|\cdot\|$ denotes a norm. The minimum number C_i satisfying the inequality (B4) is defined as the norm of the operator $\mathbf{A}_i$ and is denoted as $\|\mathbf{A}\|$. For such a definition of $\|\mathbf{A}\|$ it may be proved that

$$\|\mathbf{A}\| = \max_{\|f\| \neq 0} \frac{\|\mathbf{A}f\|}{\|f\|} \quad \text{(B5)}$$

(Kolmogorov and Fomin 1968).

If we choose to use the Hermitian norm for vectors, defined as

$$\|f\| = (|f_k^2|)^{1/2}, \quad \text{(B6)}$$

then it can be shown that the norm of any matrix $\mathbf{A}$ consistent with the definition (B5) will be given by

$$\|\mathbf{A}\| = (\|\mathbf{AA}^*\|)^{1/2} = |\lambda|_{\max}^{1/2} \quad \text{(B7)}$$

(Varga 1962).

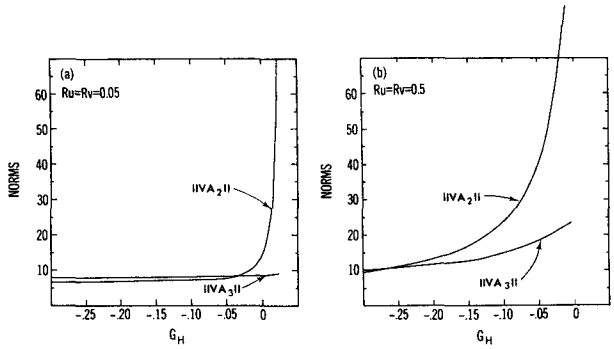

FIG. B1. Matrix norms as given by Eq. (B7) for weak (a) and strong (b) shear.

In this equation, $|\lambda|_{\max}$ is the maximum absolute value of the eigenvalues of the Hermitian matrix, $\mathbf{AA}^*$, where * means Hermitian conjugation. Equation (B7) relates a matrix norm with fundamental characteristics of the matrix such as eigenvalues and makes it advantageous over other definitions. Besides, it gives the minimum value of the constants C_i in inequality (B4) which is essential in infinitesimal expansion of Eq. (B1). Therefore, Eq. (B7) was used in the present work as a definition of a matrix norm.

The matrices, $\mathbf{VA}_y$ and $\mathbf{VA}_z$, were calculated symbolically, via REDUCE, using Eqs. (31)–(33). Their norms are functions of G_H, Ru and Rv. The range of change of G_H can be estimated from inequality (12) for stable case and from Galperin et al. (1988) for unstable case without rotation:

$$-(0.53)^2 = -0.28 \leqslant G_H \leqslant 0.0233. \qquad \text{(B8)}$$

A series of numerical evaluations of the norms, $\|\mathbf{VA}_y\|$ and $\|\mathbf{VA}_z\|$, has been performed with G_H varying in the range (B8) and for different Ru and Rv. Some of the results are shown in Fig. B1 for weak ($Ru = Rv = 0.05$) and strong ($Ru = Rv \neq 0.5$) shear. One can see that under strong stable stratification both $\|\mathbf{VA}_y\|$ and $\|\mathbf{VA}_z\|$ vary around 10. Both norms increase while approaching the range of the neutral stratification and keep growing rapidly with unstable density stratification. Under strong unstable conditions, $\|\mathbf{VA}_y\|$ reaches values about 100 and $\|\mathbf{VA}_z\|$ does not exceed 30.

REFERENCES

Andre, J. C., G. De Moor, P. Lacarrere, G. Therry and R. du Vachat, 1978: Modeling the 24 hour evolution of the mean and turbulent structures of the planetary boundary layer. *J. Atmos. Sci.*, **35**, 1861–1883.

Bradshaw, P., 1969: The analogy between streamline curvature and buoyancy in turbulent shear flow. *J. Fluid Mech.*, **36**, 177–191.

——, 1973: Effects of streamline curvature on turbulent flow. *AGARDograph*, **169**.

Clancy, R. M., K. D. Pollak and J. A. Cummings, 1988: Technical description of the optimum thermal interpolation system (OTIS) Version 1: A model for oceanographic data assimilation. FNOC Techn. Note 422-86-02, Fleet Numerical Oceanography Center, Monterey, CA.

Crawford, W. T., 1986: A comparison of length scales and decay times of turbulence in stably stratified flows. *J. Phys. Oceanogr.*, **16**, 1847–1854.

Dickey, T. D., and G. L. Mellor, 1980: Decaying turbulence in neutral and stratified fluids. *J. Fluid Mech.*, **99**, 13–31.

Dillon, T. M., 1982: Vertical overturns: a comparison of Thorpe and Ozmidov length scales. *J. Geophys. Res.*, **87**, 9601–9613.

Dougherty, J. P., 1961: The anisotropy of turbulence of the meteor level. *J. Atmos. Terr. Phys.*, **21**, 210–213.

Ellison, T. H., 1957: Turbulent transport of heat and momentum from an infinite rough plane. *J. Fluid Mech.*, **2**, 456–466.

Fernando, H., 1987: Comments on "Wind Direction and Equilibrium Mixed-Layer Depth: General Theory." *J. Phys. Oceanogr.*, **17**, 169–170.

Galperin, B., and S. Hassid, 1984: A two-layer model for the barotropic stationary turbulent planetary boundary layer. *Israel J. Technol.*, **22**, 233–242.

——, and L. H. Kantha, 1988: A turbulence model for rotating flows. *AIAA J.*, **27**, 750–757.

——, L. H. Kantha, S. Hassid and A. Rosati, 1988: A quasi-equilibrium turbulent energy model for geophysical flows. *J. Atmos. Sci.*, **45**, 55–62.

Gargett, A. E., and T. R. Osborn, 1981: Small-scale shear measurements during the Fine and Microstructure Experiment (FAME). *J. Geophys. Res.*, **86**, 1929–1944.

Garwood, R. W., 1977: An oceanic mixed-layer model capable of simulating cyclic states. *J. Phys. Oceanogr.*, **7**, 455–471.

——, 1979: Air–sea interaction and dynamics of the surface mixed layer. *Rev. Geophys. Space Phys.*, **17**, 1507–1524.

——, P. C. Gallacher and P. Muller 1985a: Wind direction and equilibrium mixed layer depth: General theory. *J. Phys. Oceanogr.*, **15**, 1325–1331.

——, P. Muller and P. C. Gallacher 1985b: Wind direction and equilibrium mixed layer depth in the tropical Pacific Ocean. *J. Phys. Oceanogr.*, **15**, 1332–1338.

Halleen, R. M., and J. P. Johnston, 1967: The influence of rotation on flow in a long rectangular channel—an experimental study. Mech. Eng. Dept., Rep. MD-18, Stanford University, Stanford, CA.

Hassid, S., and B. Galperin, 1983: A turbulent energy model for geophysical flows. *Bound.-Layer Meteor.*, **26**, 397–412.

Hopfinger, E. J., 1987: Turbulence in stratified fluids: a review. *J. Geophys. Res.*, **92**, 5287–5303.

Hunt, I. A., and P. N. Joubert, 1979: Effects of small streamline curvature on turbulent duct flow. *J. Fluid Mech.*, **91**, 633–659.

Itsweire, E. C., K. N. Helland and C. W. Van Atta, 1986: The evolution of grid-generated turbulence in a stably stratified fluid. *J. Fluid Mech.*, **162**, 299–338.

Johnston, J. P., R. M. Halleen and D. K. Lezius, 1972: Effects of spanwise rotation on the structure of two-dimensional fully developed turbulent channel flow. *J. Fluid Mech.*, **56**, 533–557.

Kantha, L. H., O. M. Phillips and R. D. Azad, 1977: On turbulent entrainment at a stable density interface. *J. Fluid Mech.*, **79**, 753–768.

——, A. Rosati and B. Galperin, 1989: Effect of rotation on vertical mixing and associated turbulence in stratified fluids. *J. Geophys. Res.*, **94**, 4843–4854.

Kato, H., and O. M. Phillips, 1969: On the penetration of a turbulent layer into a stratified fluid. *J. Fluid Mech.*, **60**, 467–480.

Klebanoff, P. S., 1954: Natl. Advisory Comm. Aeronaut. Tech. Notes No. 3178.

Kolmogorov, A. N., and S. V. Fomin, 1968: Elementy teorii funktsii i funktsionalnogo analiza. Izdatelstvo "Nauka" (in Russian)

Koyama, H., S. Masuda, I. Abriga and I. Watanabe, 1979: Stabilizing and destabilizing effects of Coriolis force on two-dimensional laminar and turbulent boundary layers. *J. Eng. Power*, **101**, 23–31.

Lakshminarayana, B., 1986: Turbulence modeling for complex shear flows. *AIAA J.*, **24**, 1900–1917.

Leuck, R., W. R. Crawford and T. R. Osborn, 1983: Turbulent dissipation over the continental slope off Vancouver Island. *J. Phys. Oceanogr.*, **13**, 1809–1818.

Martin, P. J., 1985: Simulation of the mixed layer at OWS November and Papa with several models. *J. Geophys. Res.*, **90**, 903–916.

Mellor, G. L., 1973: Analytic prediction of the properties of stratified planetary surface layers. *J. Atmos. Sci.*, **30,** 1061–1069.

——, 1975: A comparative study of curved flow and density-stratified flow. *J. Atmos. Sci.*, **32,** 1278–1282.

——, and T. Yamada, 1982: Development of a turbulence closure model for geophysical fluid problems. *Rev. Geophys. Space Phys.*, **20,** 851–875.

Miyakoda, K., and J. Sirutis, 1977: Comparative integrations of global models with various parameterized processes of subgrid-scale vertical transports. *Beitr. Z. Phys. Atmos.*, **50,** 445–487.

Monin, A. S., and A. M. Yaglom, 1971: *Statistical Fluid Mechanics: Mechanics of Turbulence.* The MIT Press, 769 pp.

Niller, P. P., 1975: Deepening of the wind mixed layer. *J. Mar. Res.*, **33,** 405–422.

Ozmidov, R. V., 1965: On the turbulent exchange in a stably stratified ocean. *Atmos. Ocean Phys.*, **8,** 853–860.

Phillips, O. M., 1977: *The Dynamics of the Upper Ocean,* second ed. Cambridge University Press, 336 pp.

Price, J. F., E. A. Terray and R. A. Weller, 1987: Upper ocean dynamics. *Rev. Geophys.*, **25,** 193–203.

Rosati, A., and K. Miyakoda, 1988: A GCM for upper ocean simulation. *J. Phys. Oceanogr.*, **18,** 1601–1626.

So, R. M. C., 1975: A turbulence velocity scale for curved shear flows. *J. Fluid Mech.*, **70,** 37–57.

Stillinger, D. C., K. N. Helland and C. W. Van Atta, 1983: Experiments on the transition of homogeneous turbulence to internal waves in a stratified fluid. *J. Fluid Mech.*, **131,** 91–122.

Varga, R. S., 1962: Matrix iterative analysis. Prentice-Hall, 322 pp.

Watmuff, J. H., H. T. Witt and P. N. Joubert, 1985: Developing turbulent boundary layers with system rotation. *J. Fluid Mech.*, **157,** 405–448.

Zeman, O., and H. Tennekes, 1975: A self-contained model for the pressure terms in the turbulent stress equations of the neutral atmospheric boundary layer. *J. Atmos. Sci.*, **32,** 1808–1813.